The g factor of conduction electrons in aluminium : calculation and application to spin resonance

Francois Beuneu

▶ To cite this version:

The g factor of conduction electrons in aluminium: calculation and application to spin resonance

F Beuneu

† Section d'Etude des Solides Irradiés. Centre d'Etudes Nucléaires. 92260 Fontenay-aux-Roses. France
and
Laboratoire de Physique des Solides (Laboratoire associé au CNRS). Université Paris-Sud, 91405 Orsay. France

Abstract. We calculate the g factor at every point of the Fermi surface of aluminium by using a classical 'four orthogonalised plane waves scheme and by introducing the spin-orbit potential as a perturbation. An important difficulty remains, linked to the choice of the wavefunction phase. Moreover we propose a phenomenological model based on the narrowing of the g distribution by two types of motion: a random one corresponding to the diffusion of electrons on the crystalline imperfections and a coherent one around the cyclotron orbits. A qualitative model accounts relatively well for the spin resonance experimental data.

1. Introduction

The conduction electron spin resonance (CESR) of aluminium has been studied extensively over the last few years. The main parameters of the resonance (g factor and linewidth) show a dependence with temperature and also with the frequency of the spectrometer which is not understood at present. In this paper we propose a phenomenological model accounting qualitatively for the experiments and based on a calculation of the g factor of Al at every point of the Fermi surface.

In two previous papers (Beuneu and Monod 1978, Monod and Beuneu 1979) we compared the CESR properties of many metals. We pointed out that the linewidth due to phonons is anomalously broad for all the polyvalent metals, and we interpreted this fact as being due to inhomogeneous spin scattering of electrons depending on their position on the Fermi surface. Such an idea makes the detailed study of the behaviour of aluminium particularly attractive. because it can lead to more understanding of the CESR properties of many non-s (polyvalent) metals.

We summarise here the main results concerning the anomalous magnetic properties of aluminium. Static susceptibility measurements (Delafond et al 1973, Mimault et al 1973) give some unexplained results: the static susceptibility is 6.3×10^{-7} EMU g^{-1} at 290 K. a value larger than the free-electron value for the Pauli susceptibility, namely 4.6×10^{-7} EMU g^{-1}. This experimental susceptibility decreases by some 30% between 10 K and 300 K. The same authors report considerable variations of susceptibility with alloying. CESR experiments in aluminium show interesting features. The

† Present address.

variation of the linewidth with temperature has been studied at a number of different frequencies: 1·27 GHz (Lubzens and Schultz 1976), 9·2 GHz (Lubzens *et al* 1972, Sambles *et al* 1977b), 21 GHz (Janssens *et al* 1975), 35 GHz (Lubzens *et al* 1972), 60 GHz (Van Meijel *et al* 1977) and 79 GHz (Dunifer and Pattison 1976). It appears from these experiments that:

(i) the linewidth is frequency dependent at all temperatures;

(ii) at a given temperature, the frequency dependence is linear, the slope decreasing by less than a factor of two from the low temperatures to 80 K (Sambles *et al* 1977a);

(iii) at frequencies larger than 10 GHz, the linewidth shows a minimum with temperature, between 20 K and 40 K.

On the other hand, the g factor varies with frequency and temperature in the 0–50 K range.

More precisely, at frequencies lower than 10 GHz the g value is frequency and temperature independent and is known to be 1·996 ± 0·001. At higher frequencies, the g value is 1·996 near 50 K but increases with decreasing temperature, the increase being faster for larger frequencies.

We have to mention here that in all these experiments there are important effects due to surface relaxation which are not understood clearly yet. Surfaces can influence CESR data in two ways: firstly, the momentum relaxation introduces motional narrowing, and secondly, the spin relaxation gives extra broadening of the lines; the two competing mechanisms give experimental data which are difficult to analyse. For a first study of surface spin relaxation in aluminium, see Sharp-Dent *et al* (1976).

The linewidth data are generally believed to be due to a g factor anisotropy over the aluminium Fermi surface. A motional narrowing mechanism would be responsible for the decrease of the linewidth with decreasing frequency and for the minimum of the linewidth with temperature at high frequencies. However, this model is unsatisfactory, as it cannot account for:

(i) the linear dependence of the linewidth with frequency (the simple motional narrowing model predicts a quadratic frequency dependence);

(ii) the small variation of the slope of this dependence with temperature (at high temperature, where the momentum collisions are very frequent, the g factor distribution should be completely narrowed, contrasting with the experimentally important variation of linewidth with frequency up to 80 K).

A more complicated model, based on many-body effects, has been proposed (Fredkin and Freedman 1972, Freedman and Fredkin 1975) but no agreement with the two points above has been obtained. From the linear frequency dependence of the linewidth, it has sometimes been proposed that there should be no motional narrowing at all in aluminium. However this hypothesis requires a scattering time of the order of 10^{-8} s, even at 80 K where the resistivity scattering time is about 10^{-13} s. This disagreement of five orders of magnitude makes nonsense of the non-motional narrowing model.

One may then consider the CESR properties of aluminium to be unexplained[†].

† Recent reports on the variations of CESR properties with frequency (in Ag and Na: Braim *et al* 1979; in Cu Stesmans *et al* 1979) seem to indicate an anomalous, aluminium-like behaviour of the linewidth with temperature and frequency. However the situation is not clear at present, as Dunifer (1980) gives results for copper which contradict those of Stesmans *et al* (1979). On the other hand, preliminary measurements on palladium metal (A Stesmans and P Monod, private communication) seem to be consistent with a very large frequency dependence of the linewidth.

It is the purpose of the present paper to give a tentative model for these properties. Our model is based on a detailed calculation of the g factor value at each point of the Fermi surface. g factor calculations are not very numerous in the literature, and most of them deal with semiconductors (Roth 1960) or semimetals (Cohen and Blount 1960). For metals we can mention calculations in alkalis (Yafet 1957, 1963, Bienenstock and Brooks 1964, Moore 1975b), iron and nickel (Singh *et al* 1976) and palladium (Lenglart 1967, Rahman *et al* 1978). Except in the last paper cited, no effort has been made to relate the calculated g factor distribution over the Fermi surface to the CESR linewidth. The only available model is that of Fredkin and Freedman (1972, see also Freedman and Fredkin 1975) which is only based on a phenomenological description of the g factor distribution. In this paper we present a model for the motional narrowing in aluminium taking into account the calculated g distribution. This phenomenological approach considers two types of motion: a random one, due to momentum scattering and a coherent one, the cyclotron motion.

2. The wavefunction of conduction electrons in aluminium

We use here a very simple method, due to Ashcroft (1963), for computing the Fermi surface of aluminium. The first step neglects the spin–orbit potential, this approximation being justified by the fact that the 3p atomic splitting due to the spin–orbit is about 10^{-3} Ryd, a value much lower than the typical band gaps in the metal. The introduction of the spin–orbit potential is made using perturbation theory, and constitutes the second step of the present section.

Ashcroft's method uses four orthogonalised plane waves (OPW) as basis functions for the description of the first conduction bands in aluminium (four is the minimum number of OPW that one must consider in order to give a satisfactory description of the Brillouin zone corner, called W, which is the point needing the greatest number of OPW). The pseudopotential is introduced phenomenologically by fitting its first Fourier components in such a way as to obtain a satisfactory picture of the Fermi surface compared with the data obtained in the de Haas–van Alphen experiments and the resulting secular equation is given in §4. At each point of the Fermi surface we compute:

(i) the wavefunction at the Fermi level, written as a linear (and normalised to unity) combination of the four OPW;

(ii) the three other energies corresponding to the three other solutions of the secular equation;

(iii) the wavefunctions for these three energy bands.

When determining this bandstructure, one finds that the point which has the coordinates $k_x = 0.9649$, $k_y = 0.4115$ and $k_z = 0$ (in $2\pi/a$ units) is quite peculiar: at this point of the Fermi surface, two energy bands are degenerate; in other words the second and third zone of the Fermi surface are in contact. This degeneracy will be lifted only by the spin–orbit and the treatment of this peculiar point is given in the appendix.

We arrive now at the point where spin–orbit perturbation must be considered. This interaction is written under the hypothesis that $V(r)$, the one-electron potential, is

spherically symmetric:

$$V_{so} = \frac{\hbar^2}{4m^2c^2} \frac{1}{r} \frac{\partial V}{\partial r} \mathbf{l}.\mathbf{s} = \lambda(r)\mathbf{l}.\mathbf{s} = \lambda(r)[l_z s_z + \tfrac{1}{2}(l_+ s_- + l_- s_+)]$$

where z is the quantisation axis and

$$l_\pm = l_x \pm il_y \qquad s_\pm = s_x \pm is_y.$$

We wish to determine how the wavefunction ψ_i (of wavevector $\mathbf{k}$) is modified with the introduction of the spin–orbit. V_{so} couples ψ_i with the other wavefunctions of the same $\mathbf{k}$, which we denote by ψ_j. Here we shall consider only the three other conduction wavefunctions obtained above in the four OPW method as ψ_j; we neglect the influence of the bands of higher order as well as the underlying levels, this being justified in a perturbation treatment by the large energy denominators linked to these bands. Following Elliott (1954) we write the wavefunction, as modified in first order in the spin–orbit perturbation, as follows:

$$\hat{\psi}_i = \psi_i|+\rangle + \tfrac{1}{2}\sum_{j \neq i}\left(\frac{\langle\psi_j|\lambda(r)l_z|\psi_i\rangle\psi_j}{E_i - E_j}|+\rangle + \frac{\langle\psi_j|\lambda(r)(l_x + il_y)|\psi_i\rangle\psi_j}{E_i - E_j}|-\rangle\right)$$

where the symbol over $\hat{\psi}_i$ denotes that this function includes the spin–orbit contribution. The form for $\hat{\psi}_i$ is no longer correct when a band j exists such that $|E_i - E_j|$ is of the order of the 3p spin–orbit splitting ($\approx 10^{-3}$ Ryd). This is the case only in the immediate neighbourhood of the point of degeneracy already mentioned (see the appendix).

We have to determine the matrix elements of the spin–orbit between two OPW. Let us write:

$$|\text{OPW}_i\rangle = (1 - P)|k_i\rangle = |k_i\rangle - \sum_\alpha |\alpha\rangle\langle\alpha|k_i\rangle$$

where the α are taken to be the 1s, 2s and 2p states of the Al^{3+} ion. Using the fact that l_z and $(1 - P)$ commute, we get:

$$\langle\text{OPW}_j|\lambda l_z|\text{OPW}_i\rangle = \langle k_j|\lambda l_z(1 - P)|k_i\rangle$$
$$= \langle k_j|\lambda l_z|k_i\rangle - \sum_\alpha \langle k_j|\lambda l_z|\alpha\rangle\langle\alpha|k_i\rangle.$$

The first term of the last expression is very small. This is rather intuitive because the spin–orbit acts principally on the core part of the wavefunction. This term will be neglected.

Writing:

$$\alpha_{nlm} = \frac{P_{nl}(r)}{r} Y_l^m(\theta, \phi)$$

where n, l and m are the classical quantum numbers associated with the core state α, and defining

$$\lambda_{nl} = \int_0^\infty \lambda(r) P_{nl}^2(r)\, dr$$

we can immediately deduce the following equation from the fact that the α are a basis of eigenfunctions for the λl_z operator:

$$\langle k_j | \lambda l_z | \alpha_{nlm} \rangle = m \lambda_{ml} \langle k_j | \alpha_{nlm} \rangle.$$

In the case of Al^{3+}, the only α to be considered, i.e. of non-zero m, are the 2p states of $m = \pm 1$. The λ_{2p} parameter will be chosen from the data corresponding to the atomic spin–orbit splittings as tabulated by Yafet (1963).

The preceding treatment of the λl_z matrix element is very similar to the one made by Asik *et al* (1969).

We have to compute the scalar products $\langle \alpha | k \rangle$ between the 2p core states and the plane waves. The calculation is done easily (see for instance Harrison 1966) by expanding the plane wave in terms of spherical harmonics and using orthogonalisation of these spherical harmonics. We obtain

$$\langle \alpha | k \rangle = \frac{4\pi}{\Omega_0^{1/2}} \, i^l \, Y_l^{m*}(\theta_k, \phi_k) \int_0^\infty j_l(kr) r P_{nl}(r) \, dr$$

where Ω_0 is the volume of the unit cell of the crystal.

Defining

$$I(k) = \int_0^\infty j_1(kr) r P_{2p}(r) \, dr$$

we obtain by a straightforward calculation:

$$\langle OPW_j | \lambda l_z | OPW_i \rangle = i\lambda_{2p} \frac{12\pi}{\Omega_0} \frac{I(k_i)}{k_i} \frac{I(k_j)}{k_j} (k_y^i k_x^j - k_y^j k_x^i).$$

The $I(k)$ integral is calculated numerically using the values of Hartree (1935) for $P_{2p}(r)$ in Al^{3+}. Values of $I(k)$ are tabulated by Beuneu (1979).

3. Calculation of the *g* factor

The problem of the Bloch electrons in a magnetic field is known to be a very complicated one: a field, even a small one, does not have a small effect on the wavefunctions because they extend to infinity throughout the crystal, and thus perturbation theory cannot be used. This difficult theoretical problem has been solved by Kohn (1959), Roth (1962) and Blount (1962). The general idea for the treatment of the magnetic field is that if the change in the wavefunctions is large, the change in the energy levels is small for ordinary fields, so that one can obtain an effective Hamiltonian where bands are decoupled.

Yafet (1963) shows in detail how such a method can be used to obtain *g* factors in crystals, following the work of Cohen and Blount (1960) for bismuth.

As a first step, consider the case of a band edge: the problem is somewhat simpler and it applies directly to semiconductors. It is useful to define a new operator, called *X*, which behaves as the periodic part of the position operator *x*. Consider two Bloch

waves Ψ_n and $\Psi_{n'}$ with periodic parts u_n and $u_{n'}$. By definition we write:

$$X_{nn'}^x = \frac{(2\pi)^3}{\Omega_0} \int_{\text{cell}} u_n^* \frac{i \partial u_{n'}}{\partial k_x} d\tau$$

where the integral is computed over the elementary cell of the crystal. The total magnetic moment can be given by

$$\mu = -\mu_B(L + \tfrac{1}{2}g_0\sigma)$$

where $g_0 = 2.0023$ is the free-electron g value. The operator L is defined by

$$L = \hbar^{-1} X \times \pi$$

where π is given by

$$\pi = p + \frac{\hbar}{4mc^2} \sigma \times \nabla V.$$

L can be interpreted as the periodic part of the angular momentum l: X being a periodic operator, its matrix elements between Bloch functions converge, and the same thing is true for L. On the contrary, neither x nor l have this property (this is clearly linked to the fact that the magnetic field cannot be treated by perturbation theory). Yafet (1957) showed that the difference between the matrix elements of X and those of x, taken over the unit cell between two Bloch functions, can be written as an integral over the surface of the unit cell; thus, if one moves the atoms of the crystal away from one another, L reduces to l in the limit of infinite interatomic distance.

With these definitions, the g factor at a band edge is shown to be

$$g = 2 \langle \psi \uparrow | L_z + 2 s_z | \psi \uparrow \rangle$$

with the condition that the matrix element of $L_z + 2 s_z$ between $\psi\uparrow$ and $\psi\downarrow$ must be zero (or negligible). Consider now a solid where the spin–orbit is small: to first order in the spin–orbit the s_z operator gives no deviation to $g = 2$, so that if we define Δg as $g - g_0$ we can write

$$\Delta g = 2 \langle \psi\uparrow | L_z | \psi\uparrow \rangle.$$

It must not be forgotten that such a formula, which neglects the non-diagonal terms in the magnetic (Zeeman) Hamiltonian, will give correct results only for $|\Delta g| \ll 2$. When the Δg is calculated at band i, it is classical to write

$$\Delta g_i = \frac{2}{\hbar} \sum_{j \neq i} (\hat{X}_{ij}^x \hat{\pi}_{ji}^y - \hat{X}_{ij}^y \hat{\pi}_{ji}^x)$$

where $\hat{X}_{ij}^x$ is a condensed form of $\langle \hat{\psi}_i | X^x | \hat{\psi}_j \rangle$.

The j index describes all the energy bands with the same wavevector, and '$j \neq i$' in the sum because $\langle \hat{\psi}_i | \pi^x | \hat{\psi}_i \rangle$ is known to be zero at a band edge.

We are now at the point when we have to consider the second step; namely, the case of the Fermi surface electrons which are not at a band edge in the metal. It is interesting to show qualitatively why this case is more complicated than the preceding one. Using a semiclassical picture, we can say that the electron velocity is zero at a band edge; on the contrary, away from a band edge, the electron has a velocity v; this

means that in a magnetic field H the electron has a cyclotron motion such that

$$v = \omega \times x = \frac{eH}{mc} \times x$$

which adds another contribution to the orbital magnetic momentum. The quantity $X_{ii}(k)$ represents a displacement of the electronic charge of a wave-packet centred in k: the magnetic moment linked to this displacement may be written as a vectorial product of X_{ii} with the electron velocity π_{ii}.

Blount (1962) and Roth (1962) have separately shown that the L contribution to the magnetic moment can be written

$$(\mu_l)_{ii} = -\mu_B \hbar^{-1}[(X \times \pi)_{ii} + X_{ii} \times \pi_{ii}]$$

which agrees with the qualitative argument given above.

This leads to the generalisation of the Δg formula given in the case of the band edge. One obtains

$$\Delta g = \frac{2}{\hbar} \sum_{j \neq i} (\hat{X}_{ij}^x \hat{\pi}_{ji}^y - \hat{X}_{ij}^y \hat{\pi}_{ji}^x) + \frac{4}{\hbar} (\hat{X}_{ii}^x \hat{\pi}_{ii}^y - \hat{X}_{ii}^y \hat{\pi}_{ii}^x).$$

There is no *a priori* reason why one of the two terms of this sum should be dominant. Our computations in aluminium, in general, give contributions of the same order of magnitude. For a detailed comment on the possible appearance of very large g factor values by using such formulae, see appendix B of the paper by Yafet (1963).

There are some important remarks which concern the Δg formula. A most surprising one is that this Δg is not unique; this is because the diagonal matrix element $\hat{X}_{ii}^x$ depends on the (arbitrary) phase of the wavefunction $\hat{\psi}_i$. This is clearly seen from the definition of $\hat{X}_{ii}^x$:

$$\hat{X}_{ii}^x = \frac{(2\pi)^3}{\Omega_0} \int_{cell} \hat{u}_i^* \frac{i\partial\hat{u}_i}{\partial k_x} \, d\tau.$$

If one changes the phase of $\hat{\psi}_i$ by a factor depending on k, one adds to X_{ii} a quantity proportional to the gradient (in k) of this factor. Thus $\hat{X}_{ii}^x$, and consequently Δg_i, are not uniquely defined. Roth (1962) and Yafet (1963) partially solved this difficulty by showing that the mean Δg over a cyclotron orbit is perfectly well defined (just because one has to integrate a gradient over a closed loop). However de Graaf and Overhauser (1969) remark that this argument is no longer satisfactory in the presence of scattering over the Fermi surface. As CESR can be observed in metal even when $\omega\tau \ll 1$ (for instance in molten Na) they deduce that $g(k)$ must be well defined. We think that this statement is much exaggerated and does not constitute any proof (see §5) but it is certain that an important and unresolved problem still remains.

As a second point, note that we shall use the approximation $\pi \simeq p$, as many authors do. In particular Roth (1962) justified this by showing that the contribution of the much neglected term to the Δg is of the order of $\langle p^2/2m \rangle/mc^2 = \langle v^2 \rangle/c^2 \ll 1$. With this approximation, we shall have no difficulty in computing the matrix elements of π between linear combinations of the OPW.

The determination of the matrix elements of the X operator is as follows. The non-diagonal matrix elements are obtained by the formula:

$$X_{ij} = -\frac{i\hbar}{m} \frac{\pi_{ij}}{E_i - E_j} \qquad \text{where} \quad i \neq j.$$

This formula is demonstrated, in the zero spin–orbit case, by Wilson (1953) and the extension to the non-zero spin–orbit case is straightforward. The diagonal matrix elements are ambiguous, as discussed above, and we have to make an arbitrary choice for the phase of $\hat{\psi}_i$. For computational simplicity, we preferred to choose ψ_i, the wavefunctions without the spin–orbit. The explicit relations obtained will be given later.

We have given above the expression of the g function relative to the wavefunction $|\hat{\psi}_i\rangle$, with quantisation along the z axis. Here we write $\Delta g = \Delta g_1 + \Delta g_2$ and compute the two terms separately. The above relation between X and π leads to

$$\Delta g_1 = -\frac{2i}{m} \sum_{j \neq i} \frac{\hat{\pi}_{ij}^x \hat{\pi}_{ji}^y - \hat{\pi}_{ij}^y \hat{\pi}_{ji}^x}{E_i - E_j}$$

which we can simplify by making the approximation $\pi \simeq p$. We must now write the $\hat{p}_{ij}$ as combinations of the p_{ij}; that is to say we introduce the spin–orbit terms explicitly. This is done by writing

$$|\hat{\psi}_i\rangle = \left(|\psi_i\rangle + i \sum_{m \neq i} \lambda_m^i |\psi_m\rangle \right) |+\rangle + |c_i\rangle |-\rangle.$$

The term $|c_i\rangle$, to first order in the λ spin–orbit, was given explicitly above. Its effect on the g shift is of second order and will be disregarded here. The term λ_m^i is written

$$\lambda_m^i = \frac{1}{2i} \frac{\langle \psi_m | \lambda l_z | \psi_i \rangle}{E_i - E_m}$$

and is a real quantity. To first order in λ one has

$$\hat{p}_{ij}^x = p_{ij}^x + i \sum_{n \neq j} \lambda_n^j p_{in}^x - i \sum_{m \neq i} \lambda_m^i p_{mj}^x.$$

It is easy to show (Beuneu 1979) that p_{ij}^x is real.

With a few manipulations we can write the expression for Δg_1 as

$$\Delta g_1 = \frac{4}{m} \sum_{j \neq i} \frac{1}{E_i - E_j} \left(\sum_{n \neq j} \lambda_n^j p_{in}^x p_{ji}^y + \sum_{m \neq i} \lambda_m^i p_{ji}^x p_{mj}^y - x \rightleftarrows y \right)$$

where '$x \rightleftarrows y$' symbolises the term obtained from the one explicitly found by permuting x and y. The last formula can easily be shown to be the one obtained by Roth (1960) using a similar treatment though she needed no term like our Δg_2 as her calculation was performed at a band edge for the cases of silicon and germanium.

Consider now the term Δg_2:

$$\Delta g_2 = \frac{4}{\hbar} \hat{X}_{ii}^x \hat{\pi}_{ii}^y - x \rightleftarrows y.$$

Although it is *not* true to write:

$$X_x |\hat{\psi}_i\rangle = X_x |\psi_i\rangle + i \sum_{m \neq i} \lambda_m^i X_x |\psi_m\rangle$$

because the X operator must be applied to λ_m^i as well, which is k dependent, the following formula can be written, always to first order:

$$\hat{X}_{ii}^x = X_{ii}^x + \mathrm{i} \sum_{m \neq i} \lambda_m^i (X_{im}^x - X_{mi}^x).$$

This formula is true because X gives only quantities which are not x-dependent with the λ_m^i term; it gives no extra contributions to the x integrals calculated when determining $\hat{X}_{ii}^x$.

X_{im}^x is given by the formula

$$X_{im}^x = -\frac{\mathrm{i}\hbar}{m} \frac{p_{im}^x}{E_i - E_m}$$

and thus is imaginary. The X_{ii}^x term is determined only when we make an arbitrary choice for the phase of ψ_i. Following Roth (1962), we impose that u_i $(r = 0)$ is real, which leads to

$$X_{ii}^x = -\mathrm{Re} \sum_{m \neq i} \frac{u_m(0)}{u_i(0)} X_{mi}^x \qquad \text{if } u_i(0) \neq 0.$$

In our case, we have just mentioned that X_{mi}^x is imaginary for $m \neq i$; the $u_m(0)$ and $u_i(0)$ terms being real by our imposed condition, we obtain $X_{ii}^x = 0$. The hypothesis $u_i(0) \neq 0$ does not seem restrictive. For a point where $u_i(0) = 0$, the property $X_{ii}^x = 0$ will be shown to be true by passing to the limit on a k space path where $u_i(0) \neq 0$. Thus we have

$$\hat{X}_{ii}^x = 2\mathrm{i} \sum_{m \neq i} \lambda_m^i X_{im}^x = \frac{2\hbar}{m} \sum_{m \neq i} \lambda_m^i \frac{p_{im}^x}{E_i - E_m}.$$

This expression carries no term of zero order in the spin–orbit.

In our first-order calculation, this enables us to replace $\hat{\pi}_{ii}^y$ by p_{ii}^y, its zero-order estimate, giving:

$$\Delta g_2 = \frac{8}{m} \sum_{m \neq i} \lambda_m^i \frac{p_{im}^x p_{ii}^y}{E_i - E_m} - x \rightleftarrows y.$$

We must not forget that one major difference between Δg_1 and Δg_2 is that the latter is somewhat arbitrary as its exact values depend on the choice of the phase, whereas Δg_1 is defined unambiguously.

4. Numerical calculation and results

The machine calculation was sufficiently simple to be performed on a desk-top calculator: the Hewlett–Packard 9825 A. In the classical 1/48th of the Brillouin zone, we have studied some 8000 points with maximum density at the places where the Fermi surface curvature is high. This Fermi surface was determined by resolving Ashcroft's equation in its reduced shape (Ashcroft 1963), taking $2\pi/a = 1$ and $\hbar^2/2m = 1$ and defining $T_i(k, E) = (k - g_i)^2 - E$:

$$(T_0 T_3 - V_{200}^2)(T_1 T_2 - V_{200}^2) - V_{111}^2 (T_0 + T_3 - 2V_{200})(T_1 + T_2 - 2V_{200}) = 0$$

with $g_0 = 0$; $g_1 = (1,1,1)$; $g_2 = (1,1,-1)$; $g_3 = (2,0,0)$ and taking Ashcroft's values (in Ryd) of $E_F = 0{\cdot}85605$; $V_{111} = 0{\cdot}0179$ and $V_{200} = 0{\cdot}0562$.

The matrix elements for the spin–orbit were computed by using the formula given in §2, with the atomic value for λ_{2p}: $\lambda_{2p} = 0{\cdot}27$ eV $= 0{\cdot}0196$ Ryd.

To determine the matrix elements of p, one has to calculate only the matrix elements between two OPW. It is reasonable to take

$$\langle \mathrm{OPW}_m | p_x | \mathrm{OPW}_n \rangle = \hbar k_x^m \delta_{mn}$$

which is true in an effective mass model. Such a model is good, as the large Δg we shall obtain are due to the magnetism of intercellular currents circulating at large distances, and *not* to contributions inside one elementary cell for which the detail of the wavefunction's core oscillations should be considered.

Thus everything is determined in the formulae giving the values of Δg_1 and Δg_2. The only thing to be specified is the direction of the quantisation axis, here labelled the z axis. We made the computations for the three simple orientations of the (100) type. It is interesting at this stage to show this theorem: at each point of the Brillouin zone, the sum of the Δg obtained for three orthogonal axes of quantisation does not depend on the choice of these axes. Consider the formulae giving Δg_1 and Δg_2. They depend on the choice of the quantisation in two ways; the first is the spin–orbit matrix elements (given in §2) and the second is the terms such as $p_{in}^x \, p_{ji}^y - x \rightleftarrows y$. The two types of term depend finally in the same manner on the choice of axes, through a term like $(k_i \times k_j)_z$. Let $S = \Delta g_x + \Delta g_y + \Delta g_z$ be the sum of the Δg with the quantisation axis along x, y and z. S is proportional to

$$\sum_{3 \text{ axes}} (k_i \times k_j)_z (k_m \times k_n)_z = (k_i \times k_j) . (k_m \times k_n)$$

which is a scalar product of vectors and thus independent of the axes chosen; the theorem is proved. This theorem has an important consequence: in a motional narrowing regime for which the observed Δg must be the mean of all the Δg around the Fermi surface, it cannot depend on the orientation of the magnetic field relative to the crystal. This is no longer the case in the event of an absence of motional narrowing.

As we wish to obtain some means of Δg we must determine the relative weight of each point of the Fermi surface. This weight must clearly be proportional to the density of states at the point k considered. If we write the four OPW secular equation of Ashcroft as $f(k, E) = 0$, the density of states is given by

$$\frac{1}{|\nabla_k E|} = \frac{|\partial f / \partial E|}{|\nabla_k f|}$$

which we estimate numerically.

The numerical results for Δg were given elsewhere (Beuneu 1979) in the form of long tables. We prefer to give a more 'visual' presentation of our results.

In figures 1–6, we show maps of the Δg values on the Fermi surface. Figures 1–3 describe the second-zone points, and figures 4–6 the third-zone points. The projection procedure used here consists of defining two numbers, called U and T, such that $k_y = U k_x$ and $k_z = T k_x$. The restriction to 1/48th of the zone leads to the inequalities $0 \leqslant T \leqslant 1$ and $T \leqslant U \leqslant 1$. These two numbers are the coordinates of the planar representations shown in figures 1–6. To be clearer, let us note that this mode of projection is obtained by taking the intersection of the vector radius ΓM (Γ being the
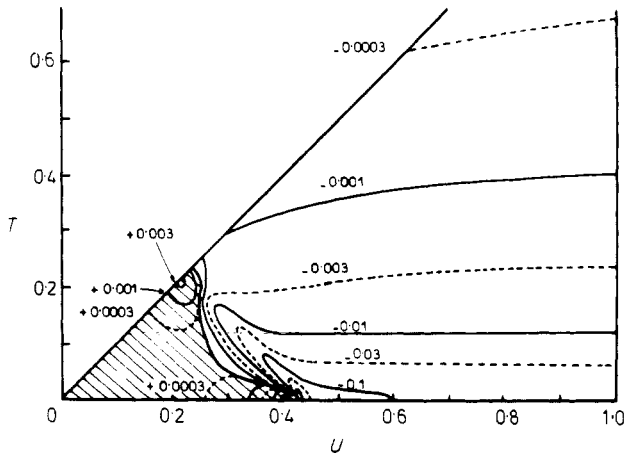
Figure 1. Reduced map of Δg in aluminium for second-zone conduction electrons at the Fermi level, in the 1/48th of the zone chosen so that $k_x \geqslant k_y \geqslant k_z \geqslant 0$. The coordinates U and T are described in the text. The magnetic field axis is taken along k_x. The shaded part of the map corresponds to the positive Δg. Note the singular point at $U = 0\cdot4265$ and $T = 0$ discussed in the appendix.

centre of the Brillouin zone and M the Fermi surface point we want to represent) with the $k_x = 1$ plane where the map is drawn. This mode of projection enables us to obtain (nearly everywhere) two distinct couples (U, T) for two distinct points on the Fermi surface taken in the same zone. For each zone, the three maps correspond to the three principal orientations of the magnetic field.

Due to the peculiar topology of the two- and three-zone volumes of the Fermi surface of aluminium, one can see that all the values of U and T correspond to a point in the second zone, and that this is not so for the 'arms' of the third zone. One property must be satisfied *a priori* by the maps: for symmetry reasons, the points in the $k_x = k_y$ plane must verify the relation $\Delta g_x = \Delta g_y$ (where the index, x or y, indicates
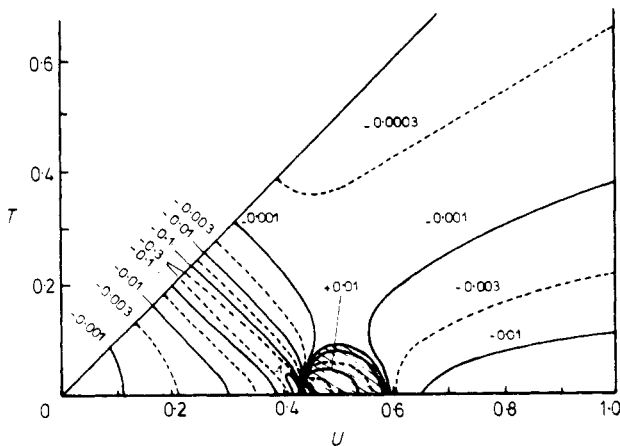

Figure 2. Reduced map of Δg in aluminium for second-zone electrons. The magnetic field axis is along k_y. The coordinates U and T are the same as for figure 1 and the projection scheme is explained in the text.
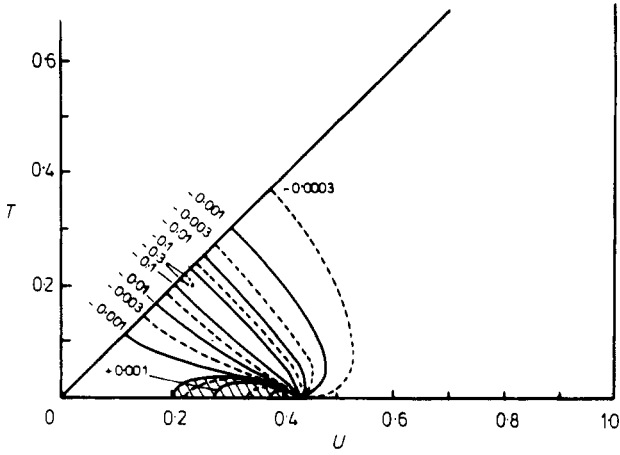
Figure 3. Reduced map of Δg in aluminium for second-zone electrons. The magnetic field axis is along k_z.
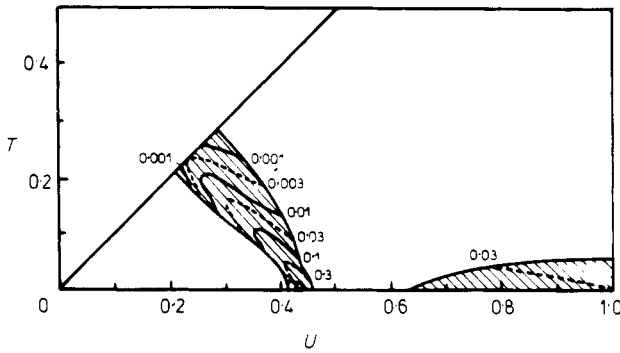

Figure 4. Reduced map of Δg in aluminium for third-zone electrons. Note that not all the couples (U, T) correspond to a third-zone point. The magnetic field axis is taken along k_x.
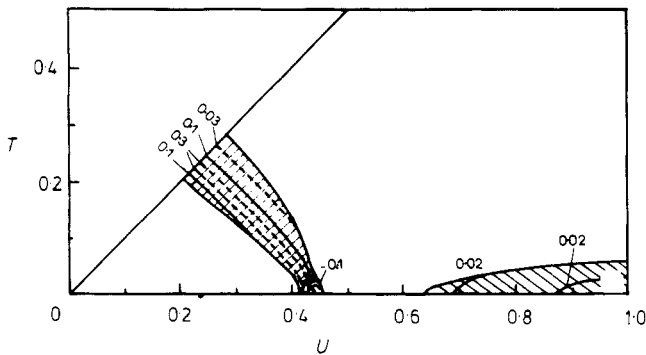

Figure 5. Reduced map of Δg in aluminium for third-zone electrons. The magnetic field axis is along k_y.
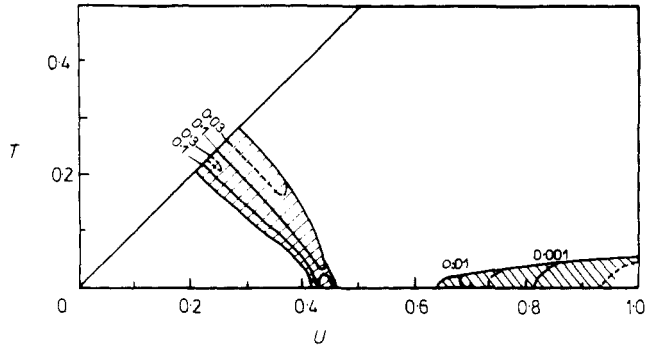
Figure 6. Reduced map of Δg in aluminium for third-zone electrons. The magnetic field axis is along k_z.

the orientation of the field). Similarly, those of the $k_y = k_z$ plane must verify that $\Delta g_y = \Delta g_z$. In other terms, the maps with field axes x and y must show the same values on the $U = 1$ line, and those with axes y and z must show the same values on the $U = T$ line. One can see in figures 1–6 that these conditions are quite well fulfilled by our calculations.

One characteristic feature of all the g factor maps is the peculiar role played by the contact point between the two zones, which is $k_x = 0.9649$, $k_y = 0.4115$ and $k_z = 0$ (in our coordinates: $U = 0.4265$ and $T = 0$). A lot of level lines converge at this point, a fact easily understood when looking at the formulae giving Δg, which include energy denominators that cancel at this point. Of course, near this point these formulae are no longer true and a special calculation concerning this is made in our appendix. However, such a treatment is needed only for a radius of approximately 2×10^{-3} (in units of U and T) around the degeneracy point, which means that our maps are true within the precision of the drawing. One can remark that there are rather large regions on the Fermi surface where the absolute value of Δg is high (for instance larger than 0.1, a very high value for such a light metal). These regions are located in the (U, T) plane, near the line of slope -1 passing by the degeneracy point just mentioned; they correspond to parts of the Fermi surface where the arms of the third zone are near to the volume of the second zone, so that there are small energy denominators involved. Also apparent on our maps is the high anisotropy of the g factor (for different field orientations, the maps are very different) and the general sign of the Δg, which is negative for most of the electrons in the second zone and positive for most in the third zone.

Note that $g(\mathbf{k})$ is not a quantity directly measurable by experiments. We wish now to present some experimentally meaningful quantities that can be deduced from our calculations. In figures 7 and 8 histograms are drawn of the Δg distribution in the second and third zones, respectively. The ordinate is proportional to the weight (as determined above) of all the Fermi surface parts having the Δg given by the abscissa. One can remark on the considerable tails of these histograms, for the negative Δg in the second zone and for the positive Δg in the third zone; for instance, 6% of the total weight of the second-zone electrons have $\Delta g < -0.1$ and 26% of the third-zone electrons have $\Delta g > +0.1$. (The relative weights of the second and third zones are 76% and 24% of the whole Fermi surface respectively. One can note here the important weight of the third-zone electrons.) These tails have considerable influence on the root
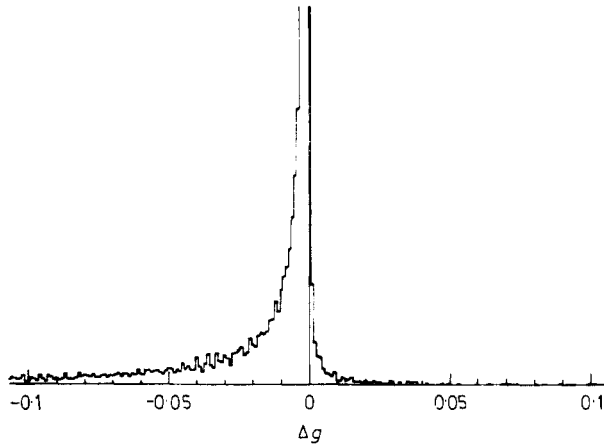
Figure 7. Histogram of $\Delta g(k)$ for each point of the Fermi surface in the second zone of aluminium. For each Δg value in the abcissa the relative weight of the part of the Fermi surface giving this Δg value is given in the ordinate. Note the large tail of the histogram for the negative Δg.

mean square (RMS) values of the Δg, which we give in the second column of table 1 for the two zones and for the whole Fermi surface, while in the first column we give the corresponding mean Δg values.

These values need some comments. The lack of uniqueness of the Δg encountered in §3 has no influence on the mean values. On the other hand, the RMS values are not uniquely defined and one may at first suspect that their very high values are due to a non-physical artefact linked to our peculiar choice of the wavefunction phases. We believe that this is not the case, because when we consider the formula $\Delta g = \Delta g_1 + \Delta g_2$, we note that only Δg_2 is badly defined; on the other hand, our calculations have shown that the histograms taken for Δg_1 and Δg_2 separately have RMS values to the same order of magnitude.
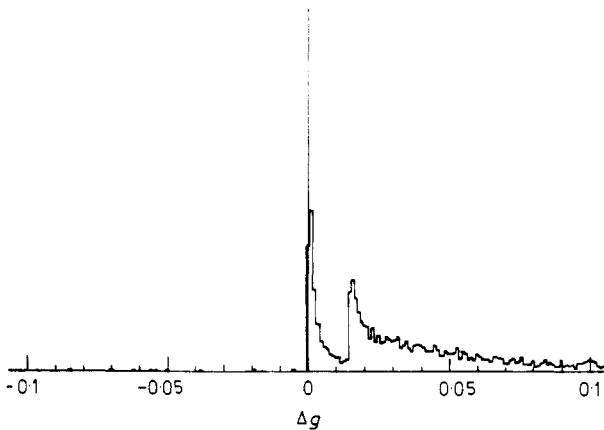

Figure 8. Histogram of $\Delta g(k)$ for each point of the Fermi surface in the third zone of aluminium. Note the large tail of the histogram for positive Δg.

Table 1. Mean and RMS values for Δg in aluminium.

| | Mean Δg | RMS Δg values | |
		$\Delta g(k)$	Δg of orbits
Second zone	−0·023	0·272	0·042
Third zone	0·078	0·815	0·071
Whole Fermi surface	0·0013	0·469	0·067

We have to comment on the mean Δg value obtained, which is $+0·001$. This value can be compared with the experimentally available Δg. For this comparison it seems coherent to consider the g value obtained when one is in a motional narrowing regime, i.e. at low frequency and 'medium' temperature (see for instance Lubzens *et al* 1972): $g = 1·996$ or $\Delta g = -0·006$.

The agreement with the calculation is very bad, as even the sign is not correctly predicted. However one must keep in mind that the total RMS value found here is 0·47 which is considerably greater than the difference between the experimental and theoretical results, making the calculated Δg rather unprecise. Furthermore, there is a contribution to Δg that has been forgotten so far: the formulae for Δg are written as sums over all the energy bands and we have restricted ourselves to the four lower conduction bands as given by the four OPW model. However one can estimate the extra contribution due to the deep-lying 2p levels of Al. For a rough order of magnitude estimate, we take $|\Delta g_{2p}| = \lambda_{2p}/\Delta E_{2p-3s}$ (Elliott 1954, Beuneu and Monod 1978) where λ_{2p} is the spin–orbit splitting of the 2p states of atomic Al (see Yafet 1963) and ΔE is the energy difference between the 2p and 3s states for atomic Al. One obtains $|\Delta g_{2p}| \approx 5 \times 10^{-3}$ which is of the order of magnitude of the difference between the experimental and theoretical Δg.

A lot of experiments in CESR in aluminium have been performed (see §1) at high frequency (and magnetic field) and low temperature. One is then in a regime where the momentum relaxation rate is much lower than the cyclotron frequency (which is equal to the Larmor frequency for $g = 2$ and $m^* = 1$). In such a case the means of Δg over the cyclotron orbits are physically relevant. We have considered 100 such orbits on the Fermi surface, with the magnetic field taken along k_z, varying k_z from 0 to 1 in $2\pi/a$ units. The mean Δg value for a given orbit is plotted against k_z in figures 9 and 10, which are drawn for the second- and third-zone electrons respectively. The quasi-degeneracy near $k_z = 0·4$ is related to the previously mentioned contact point between the two zones. In figure 11 we give new Δg histograms, which no longer concern the individual Δg (k) values (as in figures 7 and 8) but the mean Δg values over the cyclotron orbits. The striking difference between these histograms and those of figures 7 and 8 is the absence of the high Δg tails, which implies much lower RMS values for the orbital g distributions: these values are listed in the last column of table 1. One must keep in mind that the Δg over cyclotron orbits, and the RMS values of these Δg, are not phase dependent and thus are defined unambiguously.

Among the different cyclotron orbits, the extremum ones are particularly interesting. It is well known that only orbits with an extremum area can be observed by such techniques as the de Haas–van Alphen effect. These techniques sometimes allow the measurement of the mean g factor over extremum orbits, and a lot of work has been
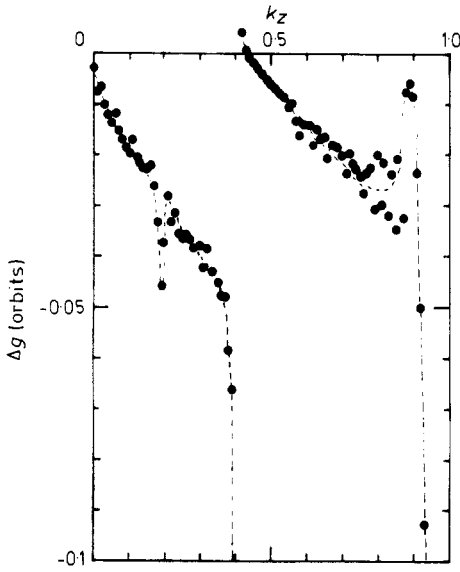
Figure 9. Mean Δg values over cyclotron orbits versus k_z, for the second zone. The full circles are calculated values and the broken curve is just to guide the eye. The discontinuity near $k_z = 0.4$ corresponds to the degeneracy point discussed in the appendix.

done in noble metals (see Randles 1972, Bibby and Shöenberg 1977, Crabtree *et al* 1977). We know of no such measurements performed in aluminium, and have found it interesting to calculate the mean g value on some extremum orbits that have been studied by the de Haas–van Alphen effect. We use the notation taken from Anderson
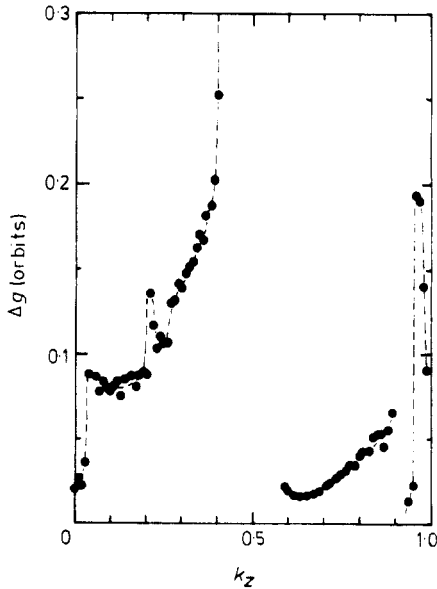

Figure 10. Mean Δg values over cyclotron orbits versus k_z, for the third zone. Note that some k_z values correspond to no third-zone points. The discontinuity near $k_z = 0.4$ corresponds to the degeneracy point discussed in the appendix.
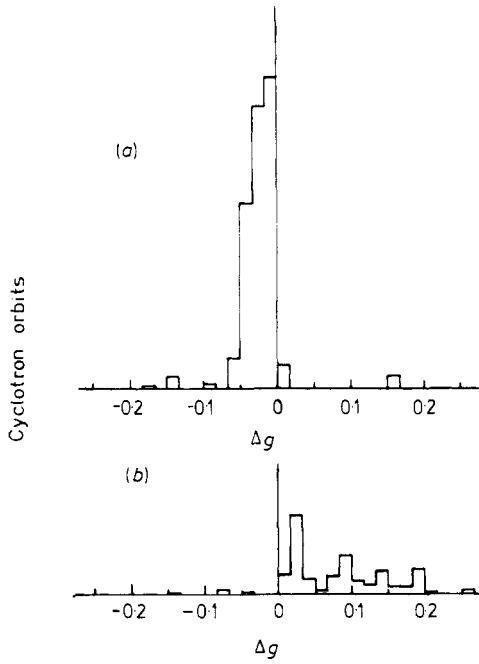
Figure 11. Histograms of the mean Δg values over cyclotron orbits, for (*a*) the second and (*b*) the third zone. The distribution tails of figures 7 and 8 are absent here.

and Lane (1970), recalled in figure 12. In table 2 we give the results of the calculations for the extremum orbits, with the corresponding field orientation.

To conclude this presentation of our calculations, we just mention that all our results are nearly unmodified by slight parameter modifications. For instance we tried the parameters proposed by Anderson and Lane (1970) which are $E_F = 0.8667$ Ryd, $V_{1\bar{1}1} = 0.018$ Ryd and $V_{200} = 0.062$ Ryd and we obtained no significant changes in Δg values and means.
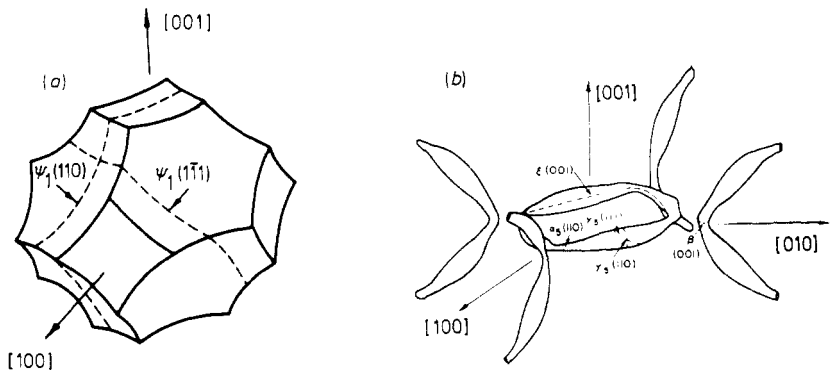

Figure 12. Main extremal orbits which can be observed in aluminium by the de Haas–van Alphen effect (Anderson and Lane 1970) in (*a*) the second and (*b*) the third zones.

Table 2.

Orbit	Orientation	Mean Δg
ψ_1	100	$-0\cdot0028$
ψ_1	110	$-0\cdot0405$
ψ_1	111	$-0\cdot0143$
β	100	$0\cdot0941$
ξ	100	$0\cdot0619$
γ_5	110	$0\cdot1423$

5. Discussion

We wish to return to the problem of the lack of uniqueness of the $g(k)$ value, as this question is as yet very unclear. We saw that in the absence of collisions, cyclotron orbits were well defined and the relevant g factors were those of the orbits, which were unambiguous. The problem arises in the presence of collisions, as de Graaf and Overhauser (1969) pointed out, and especially when $\omega\tau \ll 1$, i.e. when it is no longer possible to consider cyclotron orbits. These authors used a wave-packet treatment, leading them to g values which were independent of the wavefunction phase. Their calculation was corrected later by Moore (1975a) or, quite similarly, by Singh *et al* (1976); these treatments suppress all g factor ambiguity coming from phase problems and would modify our Δg_2 term. However this semiclassical wave-packet description was criticised by Lamb (1975) who claimed that such a model did not offer a good frame for the description of the CESR phenomena. The reason for considering this model is that one wishes to use the usual motional narrowing arguments in a regime where collisions are numerous; with the spin–orbit interaction these collisions are linked to spin-flip scattering, which becomes mixed in a complex fashion with the radio-frequency spin-flipping. Lamb's opinion is that any wave-packet approach implicitly ignores this problem and cannot account for the CESR in a rigorous way. This complicated controversy means that the problem is still open. However our feeling is that individual $g(k)$ need *not* be well defined, as they are not physically observable quantities. One has only to propose a narrowing mechanism such that the finally observable quantity be defined uniquely. The only tentative approach in this direction is that of Lamb (1975) and is restricted to the case when $\omega\tau \gg 1$. We shall not propose any answer to the problem in the general case. We believe that a way of approaching the $\omega\tau \ll 1$ case is as follows. In a $k \rightarrow k'$ collision the phaseshift is well defined and may be calculated for simple cases. This imposes one condition between the *a priori* arbitrary phases of the k and k' wavefunctions. As each collision introduces such a phase relation, we hope that it is possible to avoid the ambiguity problem even in the case where the collisions are numerous ($\omega\tau \ll 1$).

From the above considerations, it is clear that the model which we present now cannot be considered as rigorous; we will give only qualitative arguments whose purpose is to explain most of the strange CESR properties of aluminium. As we explained in §1, we consider it obvious that aluminium electron spins are in a motional narrowing regime. A further argument can be taken from the RMS value of g, called σ_g hereafter, that can be deduced from the slope of ΔH versus frequency, under the hypothesis of no motional narrowing: $\sigma_g = 0\cdot0088$. This value is considerably

lower than the 0·067 value computed here in the cyclotron motion regime, which does not seem to be understandable. In the simple motional narrowing theory (see for instance Pines and Slichter 1955) one can write:

$$\tfrac{1}{2}\Delta H = \gamma^{-1}\Delta\omega^2\tau = \gamma^{-1}\tfrac{1}{4}\sigma_g^2\omega^2\tau$$

where τ is the momentum relaxation time, which will be taken as the resistivity lifetime. Here ΔH is only the part of the CESR linewidth due to g factor anisotropy: the linewidth due to spin relaxation has been subtracted. We showed in §1 why this model cannot account for the CESR properties of aluminium: the experimental law is linear with frequency and shows only slight dependence on temperature (i.e. on τ). Our idea is that these difficulties are due to the cyclotron motion being forgotten in such a simple model, but it must cause some narrowing in a different way to a random walk motion.

We found it simple to treat this problem as follows. Starting with the simple motional narrowing formula just given above, we suppose that σ_g varies with $\omega\tau$. Note that we take in this extremely simplified model a unique cyclotron frequency, supposed to be equal to the Larmor frequency ω. For $\omega\tau \gg 1$, a conduction electron travels around its cyclotron orbit for a long time before being diffused, so that the g factor distribution of this orbit is completely narrowed. For this regime it is then natural to take $\sigma_g = 0·067$, computed above for the Δg of the orbits. This is equivalent to the results obtained on a more rigorous basis by Lamb (1975). In the opposite regime, $\omega\tau \ll 1$, the cyclotron motion can be neglected because of the rapid random diffusion over the Fermi surface. We shall take $\sigma_g = 0·47$ here which is the RMS value obtained for the individual $g(\mathbf{k})$. We now choose a completely arbitrary interpolation law between the two regimes, imposing $\sigma_g = \alpha(\omega\tau)^{-1/2}$ between the two extreme values for σ_g. In this intermediate regime we obtain:

$$\tfrac{1}{2}\Delta H = \frac{\alpha^2}{4\gamma}\frac{\omega^2\tau}{\omega\tau} = \frac{\alpha^2}{4\gamma}\omega.$$

We have chosen the law for σ_g such that ΔH varies linearly with ω. The interesting feature, which is not trivial, is the disappearing of τ: in this extremely simple model, ΔH does not vary with temperature (keeping in mind that here we forget the spin relaxation contribution adding to ΔH in practice).

In figure 13 we give the variation of the CESR linewidth of aluminium (always forgetting the phonon spin relaxation) with frequency for a wide range of scattering time τ, as can be predicted by our model. The linear parts of the curves have been given a reasonable slope by fitting the parameter α mentioned above. One can see that for τ ranging from 3×10^{-13} s to 10^{-11} s the curves obtained show an important linear part. These τ values have reasonable orders of magnitude over the 0–80 K temperature range. Moreover the parabolic rise above 50 GHz shown in figure 13 by the curve $\tau = 10^{-11}$ s agrees with the experimental deviation from linearity observed by Dunifer and Pattison (1976) at low temperature.

There is a complementary method for testing our model[†]. In the motional narrowing formula

$$\tfrac{1}{2}\Delta H = \tfrac{1}{4}\gamma^{-1}\sigma_g^2\omega^2\tau$$

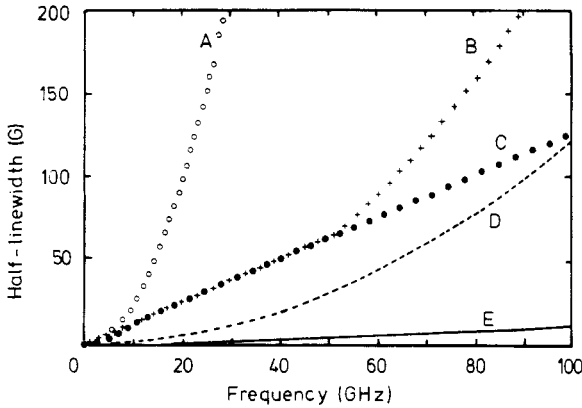[†] We are indebted to Professor W Kohn who suggested this approach.

Figure 13. Predicted CESR linewidth of aluminium versus frequency. Spin relaxation has been omitted and should be added to the frequency-dependent width. Our model predicts different behaviour for different values of the scattering time τ; the curves correspond to the following τ values: A, 10^{-10} s; B, 10^{-11} s; C, 10^{-12} s; D, 10^{-13} s; E, 10^{-14} s.

every quantity except σ_g is accessible experimentally (with a large indeterminate ω and τ). It is thus possible to plot the experimental variation of σ_g with ω and τ. This is done in figure 14, taking the easily attainable parameter F/ρ as a representation of $\omega\tau$ (where F is the CESR frequency and ρ the resistivity of the sample at different temperatures). The conclusions are that σ_g varies quite like $(\omega\tau)^{-1/2}$, and figure 14 also shows that $\omega\tau$ is a good parameter with which to define σ_g; we obtain the same σ_g for different ω and τ having the same $\omega\tau$ value. On the other hand, the regimes $\omega\tau \gg 1$ and $\omega\tau \ll 1$ are badly described, particularly for $\omega\tau \ll 1$ where σ_g exceeds the calculated maximum value ($\sigma_g = 0.47$). We note that this regime corresponds to the high-temperature range when the spin-flip due to phonons makes data analysis particularly difficult.

It is interesting to note that Fredkin and Freedman (1972) have considered, as we did here, the influence of the cyclotron motion on the linewidth, which is expressed by their formula (4). However they probably considered the effect to be unimportant because they were not aware of the large difference between the two extreme values of σ_g found by us. The simplest form of their formula (4) gives:

$$\sigma_g = \left(G_1 + \frac{G_2}{1 + \omega^2\tau^2} \right)^{1/2}.$$

This expression for σ_g has qualitatively the same behaviour as the empirical one used above: σ_g is constant for very high and very low values of $\omega\tau$, and there is an intermediate regime where σ_g decreases with increasing $\omega\tau$. However such a law will not ensure a linear ΔH versus frequency law. However one must keep in mind that τ is a very badly defined quantity. Wegehaupt and Doezema (1978) measured a very high anisotropy of τ over the Fermi surface, and this complication made any comparison difficult between the simple formulae obtained with the hypothesis that τ is isotropic, and experiment.

We have not discussed so far the experimental variation of g with temperature and

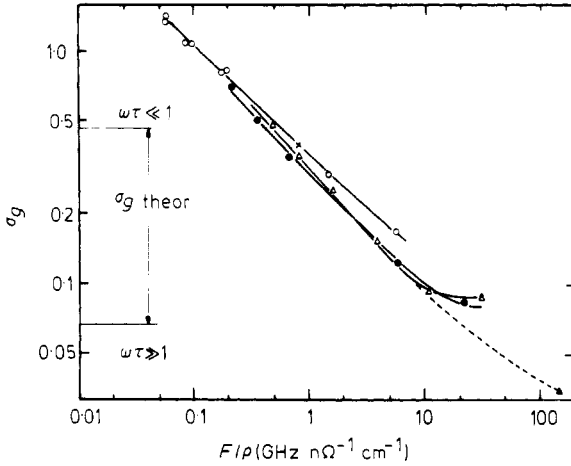**Figure 14.** σ_g values taken from experiment and with the assumption of simple motional narrowing, versus the ratio of frequency to resistivity. This ratio approximately describes the product $\omega\tau$. The curves relate the points corresponding to a given sample measured at a given frequency ($\times$, 1·27 GHz; $\bigcirc$, 9·2 GHz; $\bullet$, 35 GHz; $\triangle$, 79 GHz (27 μm); $\blacktriangle$, 79 GHz (132 μm)) and at different temperatures. The theoretical σ_g values in the two limits $\omega\tau \gg 1$ (narrowing by orbital motion) and $\omega\tau \ll 1$ (narrowing by collisions) are included.

frequency in aluminium. In principle, it is not necessary to invoke Fermi liquid effects to account for this variation, because the g factor distribution is not symmetric around its mean. However we shall show that these effects, described by Fredkin and Freedman (1972), give a good order of magnitude for the g shifts. The authors find that

$$\Delta g = \frac{X^2}{1 + X^2} \frac{(1 + B)^2 \sigma_g^2}{2B} \qquad \text{with } X = \frac{B\omega\tau}{1 + B}.$$

Again imposing $\sigma_g = \alpha(\omega\tau)^{-1\cdot 2}$ and taking $X^2 \ll 1$ and $B \ll 1$ we obtain

$$\Delta g = \tfrac{1}{2}B\alpha^2 \omega\tau.$$

Dunifer *et al* (1977) determined $B = +0\cdot 1$ by observing spin waves in aluminium. For $\tau = 2 \times 10^{-11}$ s we find $\Delta g = 0\cdot 004$ at 35 GHz and $0\cdot 010$ at 79 GHz; for samples of resistivity giving such a τ value, one has $\Delta g = 0\cdot 009$ at 35 GHz and $0\cdot 012$ at 79 GHz (Lubzens and Schultz 1976, Dunifer and Pattison 1976). The agreement is qualitatively correct at both frequencies, although non-qualitatively correct at 35 GHz.

In conclusion, we believe that the idea of a double type of motional narrowing (from a coherent and a random motion) is the relevant one for understanding the strange CESR properties of aluminium. We obtained, with very simplified models, qualitative agreement with experiments. We think that it would be necessary to take into account the anisotropy of τ (and of the cyclotron frequency) in order to obtain quantitative agreement. However our model is unable to explain the anomalous value of the static susceptibility of aluminium. On the other hand we hope that the mechanism of narrowing described here will help to understand the CESR properties of other complex metals.

Acknowledgments

Appendix. Treatment of the point of degeneracy

The point of reciprocal space with coordinates $k_x = 0.9649$, $k_y = 0.4115$ and $k_z = 0$ is a point where two energy bands intercept at the Fermi level. As the spin–orbit lifts the degeneracy at this point, it cannot be treated by the perturbation scheme developed in §2. We wish to give here, in the vicinity of this contact point between the second and third zones, some indications of the treatment leading to the g factor. For a detailed account, see Beuneu (1979).

   The part of the Fermi surface for which the general calculation of §2 is no longer valid is quite small; it corresponds to those points where the energy gap is smaller than the spin–orbit splitting of the 3p states, which is approximately 10^{-3} Ryd. In such a region we can neglect the two bands (obtained in the four OPW model) which are not in the vicinity of the Fermi level. Let ψ_1 and ψ_2 be the nearly degenerate wavefunctions calculated using the Ashcroft model (without the spin–orbit). Introducing the spin–orbit leads to a secular equation which is a 4×4 determinant, with basis functions $\psi_1\uparrow$, $\psi_2\uparrow$, $\psi_1\downarrow$ and $\psi_2\downarrow$.

   From this equation one can determine the wavefunctions (with the spin–orbit) and apply the Δg formulae given in §3. Let ΔE be the energy splitting due to the spin–orbit; its order of magnitude is 10^{-3} Ryd. Defining

$$iA = \tfrac{1}{2}\langle \Psi_1 | \lambda(r)l_z | \Psi_2 \rangle$$

with A real we get for Δg_1:

$$\Delta g_1 \simeq \frac{4}{m} \frac{A}{(\Delta E)^2} [\langle \psi_1 | p_x | \psi_2 \rangle (\langle \psi_1 | p_y | \psi_1 \rangle - \langle \psi_2 | p_y | \psi_2 \rangle) - x \rightleftarrows y].$$

The formula for Δg_2 is more complicated and will not be reproduced here.

   We wish here only to estimate the order of magnitude of Δg around the contact point. Taking $\Delta E \simeq 10^{-3}$ Ryd near this point and considering all the matrix elements of p to be of the order of unity, we obtain a value of a few hundred for Δg. On the other side we have calculated the relative weight of those points on the Fermi surface for which $|E(\Psi_1) - E(\Psi_2)| < 10^{-3}$ Ryd and found nearly 5×10^{-6} for each zone. The variation of the mean Δg due to the degeneracy point is thus of the order of 10^{-3}; furthermore it should be noted that the signs of Δg are opposite for the two zones.

References

Anderson J R and Lane S S 1970 *Phys. Rev.* B **2** 298–308
Ashcroft N W 1963 *Phil. Mag.* **8** 2055–83

Asik J R, Ball M A and Slichter C P 1969 *Phys. Rev.* **181** 645–61
Beuneu F 1979 *PhD Thesis* Orsay University, France (Rapport CEA R-5026)
Beuneu F and Monod P 1978 *Phys. Rev.* B **18** 2422–5
Bibby W M and Shöenberg D 1977 *Phys. Lett.* **60A** 235–6
Bienenstock A and Brooks H 1964 *Phys. Rev.* **136** A784–802
Blount E I 1962 *Phys. Rev.* **126** 1636–53
Braim S P, Sambles J R, Cousins J E, Van Meijel J, Stesmans A and Witters J 1979 *Solid St. Comun.* **29** 621–4
Cohen M H and Blount E I 1960 *Phil. Mag.* **5** 115–26
Crabtree G W, Windmiller L R and Ketterson J B 1977 *J. Low. Temp. Phys.* **26** 755–62
Delafond J, Junqua A and Mimault J 1973 *Phys. Stat. Solidi* **15** 553–8
Dunifer G L 1980 to be published
Dunifer G L and Pattison M R 1976 *Phys. Rev.* B **14** 945–50
Dunifer G L, Pattison M R and Hsu T M 1977 *Phys. Rev.* B **15** 315–22
Elliott R J 1954 *Phys. Rev.* **96** 266–79
Fredkin D R and Freedman R 1972 *Phys. Rev. Lett.* **29** 1390–3
Freedman R and Fredkin D R 1975 *Phys. Rev.* B **11** 4847–58
de Graaf A M and Overhauser A W 1969 *Phys. Rev.* **180** 701–6
Harrison W A 1966 *Pseudo-potentials in the Theory of Metals* (New York: Benjamin)
Hartree D R 1935 *Proc. R. Soc.* A **151** 96–105
Janssens L, Stesmans A, Cousins J E and Witters J 1975 *Phys. Stat. Solidi* b **67** 231–7
Kohn W 1959 *Phys. Rev.* **115** 1460–78
Lamb W J 1975 *PhD Thesis* University of California
Lenglart P 1967 *J. Phys. Chem. Solids* **28** 2011–25
Lubzens D and Schultz S 1976 *Phys. Rev. Lett.* **36** 1104–6
Lubzens D, Shanabarger M R and Schultz S 1972 *Phys. Rev. Lett.* **29** 1387–90
Mimault J, Delafond J and Junqua A 1973 *Phys. Stat. Solidi* **20** 195–200
Monod P and Beuneu F 1979 *Phys. Rev.* B **19** 911–6
Moore R A 1975a *J. Phys. F: Metal Phys.* **5** 459–67
——1975b *J. Phys. F: Metal Phys.* **5** 2300–6
Pines D and Slichter C P 1955 *Phys. Rev.* **100** 1014–20
Rahman T S, Parlebas J C and Mills D L 1978 *J. Phys. F: Metal Phys.* **8** 2511–24
Randles D L 1972 *Proc. R. Soc.* A **331** 85–101
Roth L M 1960 *Phys. Rev.* **118** 1534–40
——1962 *J. Phys. Chem. Solids* **23** 433–46
Sambles J R, Cousins J E, Stesmans A and Witters J 1977a *Solid St. Commun.* **24** 673–6
Sambles J R, Sharp-Dent G, Cousins J E, Stesmans A and Witters J 1977b *Phys. Stat. Solidi* b **79** 645–54
Sharp-Dent G, Hardiman M, Sambles J R and Cousins J E 1976 *Phys. Stat. Solidi* b **75** 155–61
Singh M, Callaway J and Wang C S 1976 *Phys. Rev.* B **14** 1214–20
Stesmans A, Van Meijel J and Braim S P 1979 *Phys. Rev.* B **19** 5470–4
Van Meijel J, Stesmans A and Witters J 1977 *Solid. St. Commun.* **21** 753–5
Wegehaupt T and Doezema R E 1978 *Phys. Rev.* B **18** 742–8
Wilson A H 1953 *The Theory of Metals* (London: Cambridge University Press)
Yafet Y 1957 *Phys. Rev.* **106** 679–84
——1963 *Solid St. Phys.* **14** 1–98